Molecular Cell, Volume *71*

Supplemental Information

Architectural Proteins and Pluripotency Factors Cooperate to Orchestrate the Transcriptional Response of hESCs to Temperature Stress

Xiaowen Lyu, M. Jordan Rowley, and Victor G. Corces

SUPPLEMENTAL INFORMATION

Architectural proteins and pluripotency factors cooperate to orchestrate the transcriptional response of hESCs to temperature stress

Xiaowen Lyu[1], M. Jordan Rowley[1], and Victor G. Corces[1]

SUPPLEMENTAL FIGURES

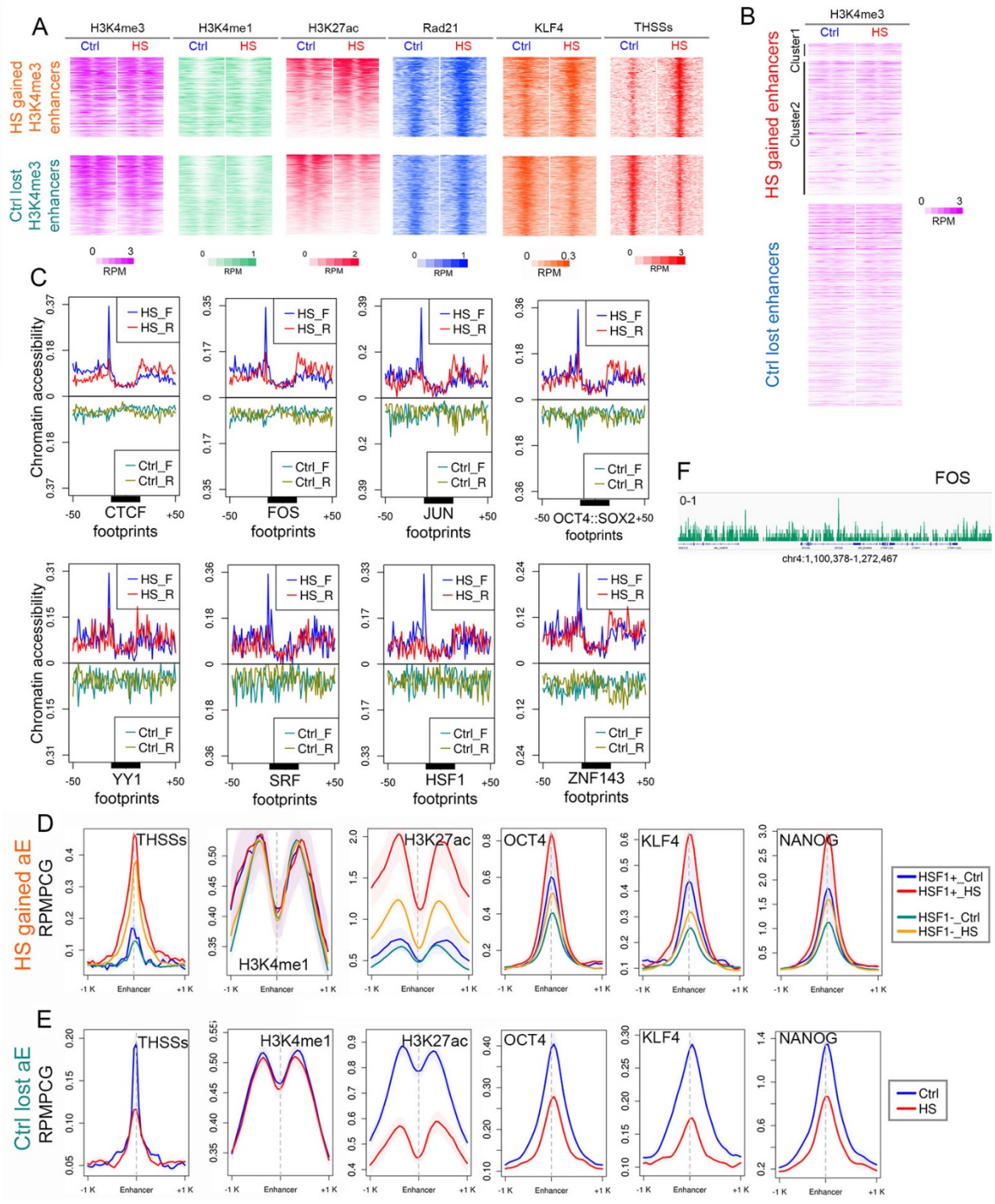

Figure S1. Related to Figure 1.

(A) Heatmaps showing changes induced after temperature stress for H3K4me3, H3K4me1, H3K27ac, RAD21, KLF4, and ATAC-seq THSSs, at HS gained enhancers defined based on the

presence of H3K4me3 ChIP-Seq signals ±1 kb of enhancer summit (upper panels). Changes of the same features at Ctrl lost enhancers are shown in the lower panels. RPM: reads per million per 50 bp bin.
(B) Heatmaps showing changes in H3K4me3 at enhancers defined in Figure 1C based on the presence of H3K4me1 at HS gained enhancers based on ChIP-Seq signals ±1 kb of enhancer summit (upper panels). Changes of H3K4me3 at Ctrl lost enhancers are shown in the lower panels. RPM: reads per million per 50 bp bin.
(C) Analysis of transcription factor motifs found at enhancers activated after temperature stress. Average profiles of ATAC-seq signal (<115 bp) at TF motifs show gain of footprints after temperature stress.
(D) Average profiles of ChIP-seq signals for ATAC-seq THSSs, H3K4me1, H3K27ac, OCT4, KLF4, and NANOG at HSF1+ and HSF1- HS-gained enhancers. RPMPCG: reads per million per 50 bp covered bin. Shading indicates 95% confidence intervals estimated by non-parametric bootstrapping.
(E) Average profiles of ChIP-Seq signals for ATAC-seq THSSs, H3K4me1, H3K27ac, OCT4, KLF4, and NANOG at enhancers that become decommissioned after temperature stress. RPMPCG: reads per million per 50 bp covered bin.
(F) Example of FOS ChIP-seq signal at a random genomic region.

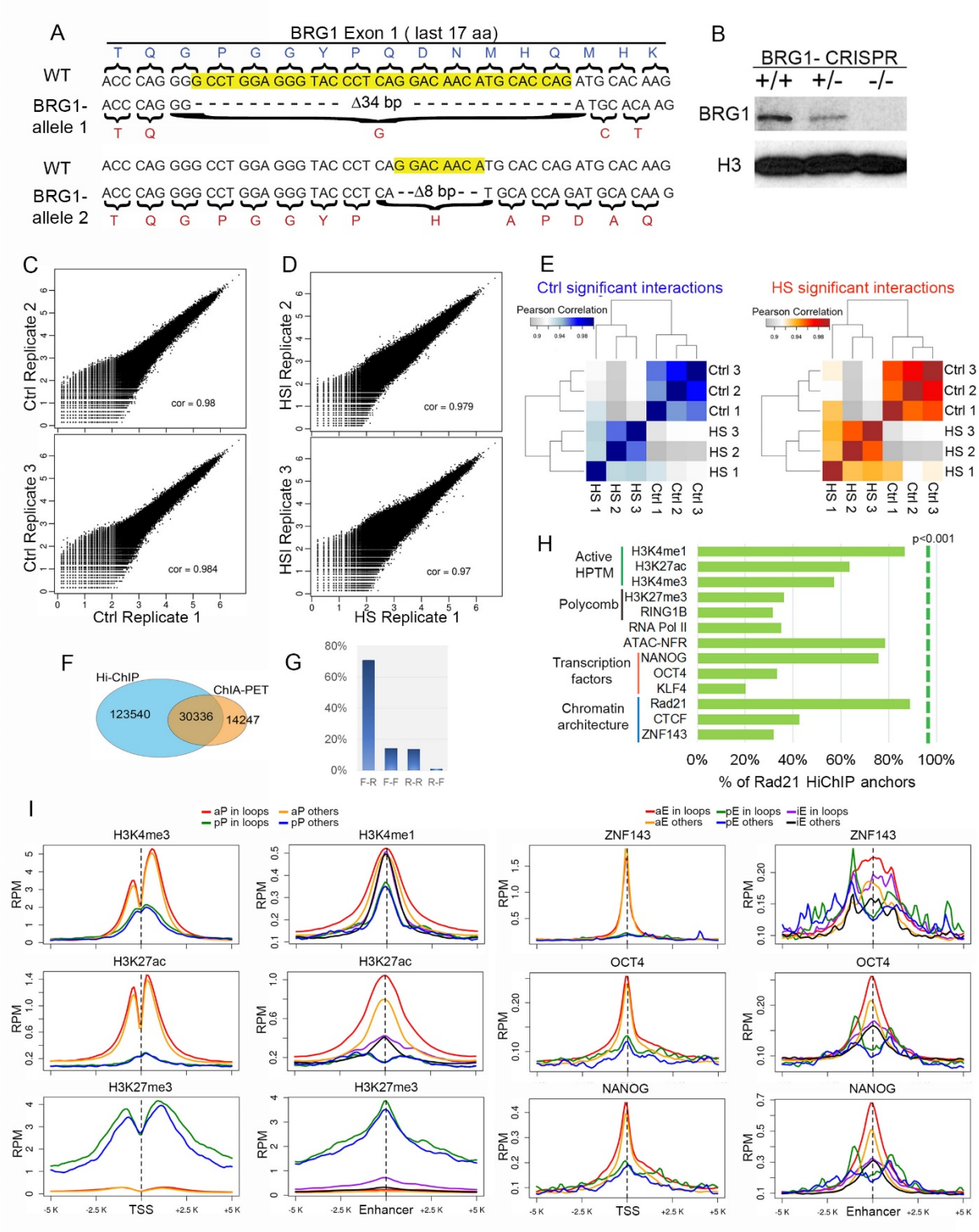

Figure S2. Related to Figure 2 and Figure 3.

(A) Diagram showing BRG1-/- frameshift mutations in exon 1 obtained by CRISPR in both alleles and the corresponding translated products.

(B) Western blot confirming depletion of BRG1 in mutant cells.

(C) Scatter plots showing Pearson's correlation of three biological replicates of Ctrl RAD21 HiChIP libraries of H9 hESCs. Interaction reads in 10 kb bins are log transformed.
(D). Scatter plots showing Pearson's correlation of three biological replicates of HS RAD21 HiChIP libraries. Interaction reads in 10 kb bins are log transformed.
(E) Clustered heatmaps showing Pearson's correlation of interactions reads density in 10 kb bins of all Ctrl and HS biological replicates on Ctrl and HS significant interactions. Clustering method is hierarchical complete linkage.
(F) Venn diagram showing overlap of significant interactions from Rad21 HiChIP and published Rad21 ChIA-PET. Rad21 ChIA-PET is from WIBR2 hESCs.
(G) Ratio of CTCF motif orientations in all CTCF/cohesin loops.
(H) Percentage of Rad21 HiChIP anchors overlapping with distinct chromatin states and proteins based on ChIP-seq data. Dashed lines indicate significant p values over random genome background.
(I) Related to Figure 3. Average profiles of different proteins at promoters and enhancers complementing those shown in Figure 3F. RPM: reads per million per 50 bp bin.

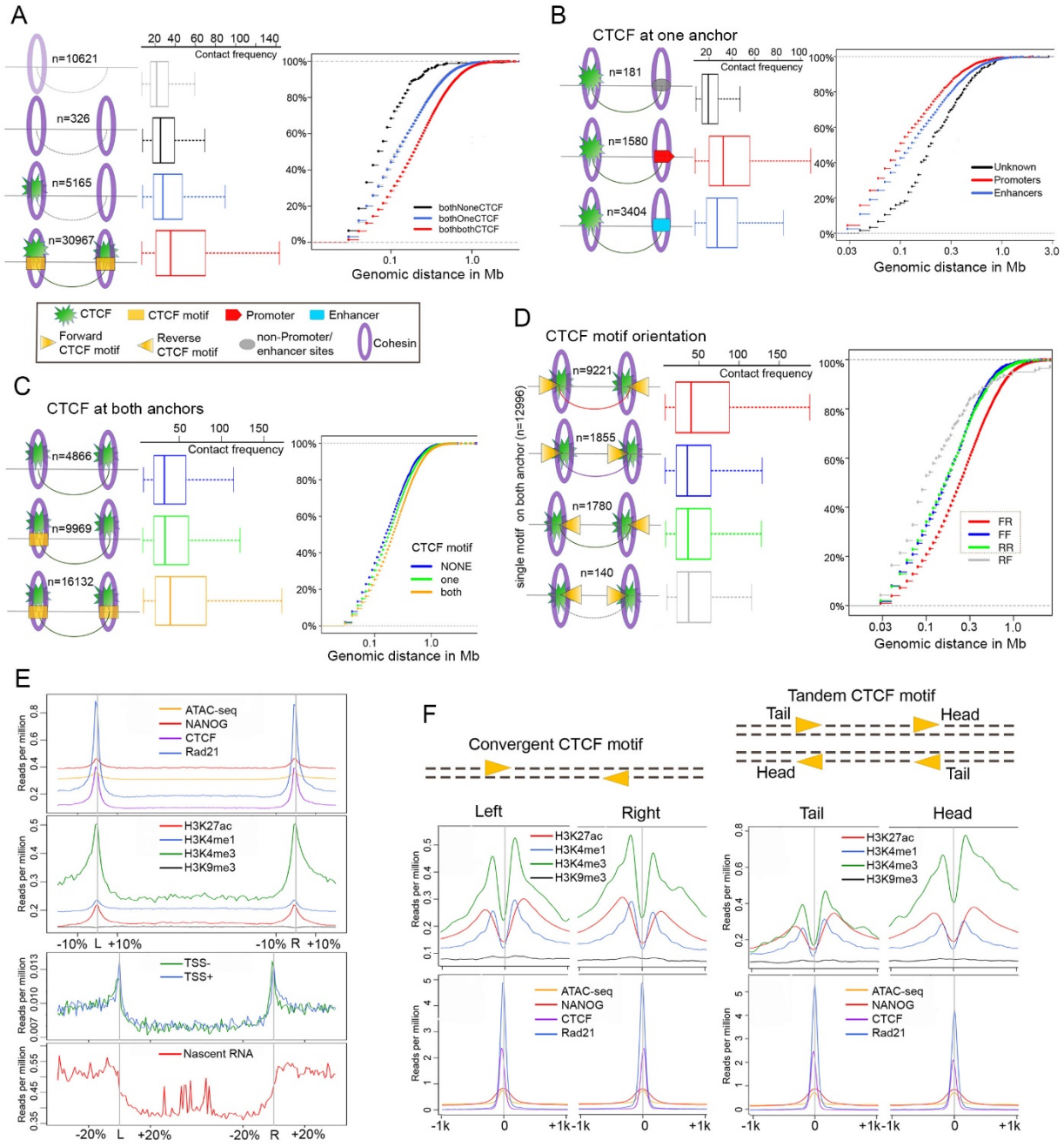

Figure S3. Related to Figure 3.

(A) Statistical analyses of cohesin loops with CTCF on neither, either or both anchors. Contact strength and genomic span for each group of loops are also compared based on Rad21 HiChIP. Loops were called using HiCCUPS.

(B) Number of CTCF loops in (A) with enhancers or promoters at the other anchor. Contact strength and genomic span for each group of loops are also compared based on Rad21 HiChIP.

(C) Number of CTCF loops in (B) with CTCF motifs on neither, either or both anchors. Contact strength and genomic span for each group of loops are also compared based on Rad21 HiChIP.

(D) Summary of CTCF motif orientations at CTCF loop anchors in (C). Contact strength and genomic span for each group of loops are also compared based on Rad21 HiChIP.

(E) Average profiles of ChIP-Seq of NANOG, H3K4me3, H3K4me1, H3K9me3, and H3K27ac, ChIP-Nexus of CTCF and Rad21, ATAC-seq NFR reads, annotated gene TSSs on both strands, and nascent RNA sequencing data obtained by EU-seq on size-scaled CTCF-CTCF loops. Regions -20% and +20% scaled relative to loop span are also included.
(F) Zoomed in view of CTCF anchors ±2 kb of CTCF-CTCF loops. Schematics of CTCF motif orientation at loop anchors are plotted on top of average profiles of data used in (E).

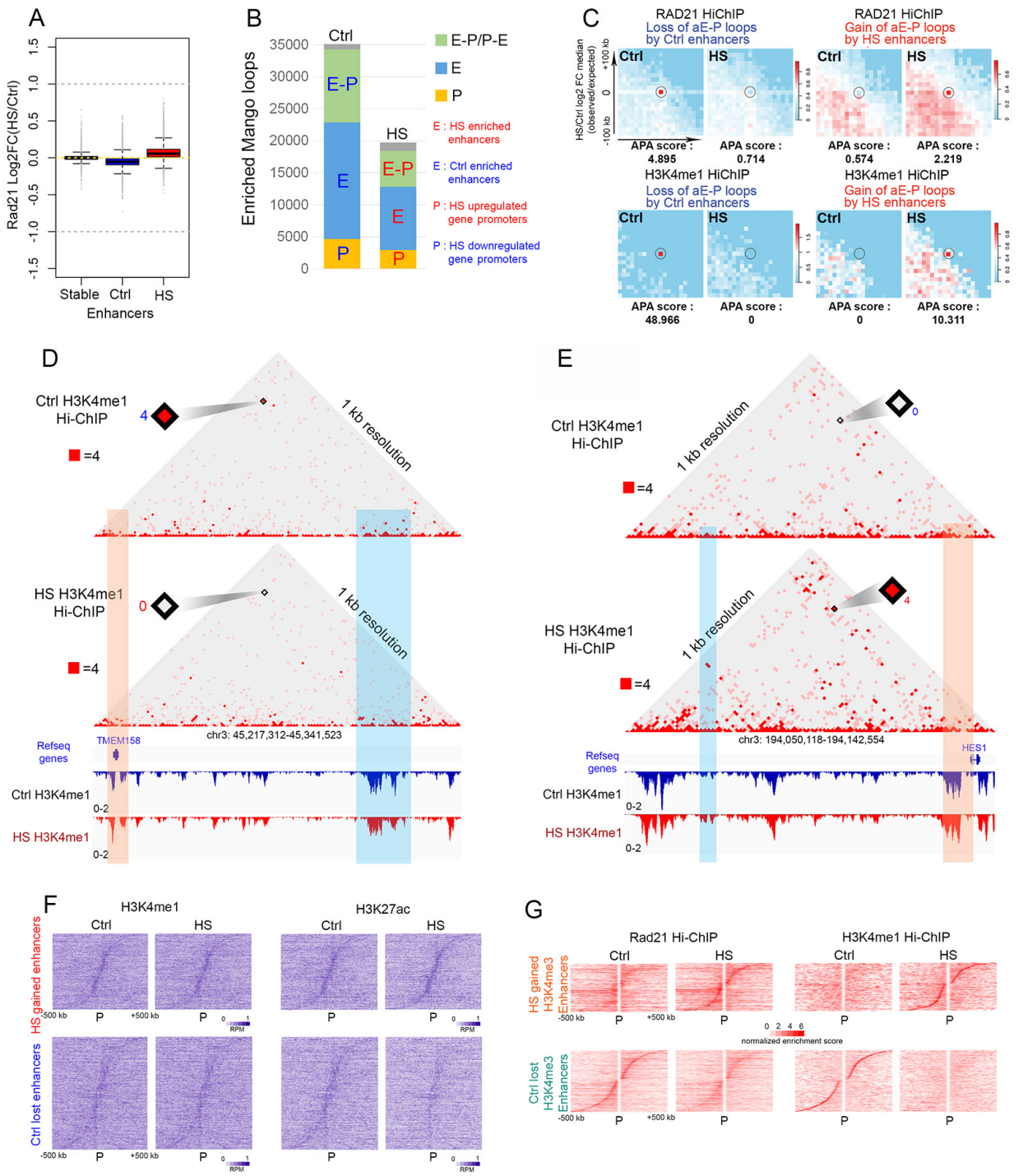

Figure S4. Related to Figure 4.

(A) Box plots comparing signal changes in Rad21 ChIP-seq between Ctrl and HS on Stable, Ctrl-enriched and HS-enriched enhancers shown in Figure 1C. Log2FC: fold changes in log2.

(B) Bar plot showing the number of Ctrl enriched RAD21 loops mediating contacts enriched in enhancers and promoters in Ctrl cells, and of HS enriched RAD21 loops mediating contacts enriched in enhancers and promoters in HS cells.

(C) APA metaplots showing HS-induced loss of aggregate signal on all loops between Ctrl lost active enhancers and HS-repressed genes (upper left two) and HS-induced gain of aggregate

signal between HS gained active enhancers and HS-induced genes (upper right two) based on RAD21 HiChIP. Similar effects are observed in APA matrices calculated from H3K4me1 HiChIP. APA matrices are made in 10 kb bin, loop anchors ± 10 bins (100 kb) regions are shown. APA scores are listed under APA plots. Color scale blue-white-red indicates increase of aggregate signals, red is higher than white, white is higher than blue.
(D) Juicebox view of read-normalized Ctrl and H3K4me1 HiChIP in the same region shown in Figure 4A (chr3: 45,217,312 - 45,341,523) containing the HS-repressed gene TMEM158. Orange vertical stripe highlights the TMEM158 genic region; blue vertical stripe highlights region containing an enhancer whose interaction is lost after temperature stress (see Figure 4A).
(E) Juicebox view of read-normalized Ctrl and HS H3K4me1 HiChIP on the same region shown in Figure 4B (chr3:194,050,118 - 194,142,554) containing the HS-induced gene HES1. Orange vertical stripe highlights HES1 genic region; blue vertical stripe highlights its gained interacting enhancers in HS (see Figure 4B).
(F) Heatmaps comparing changes in ChIP-seq signal for H3K4me1 and H3K27ac at HS gained and control lost enhancers. Only interactions within 500 kb are plotted. Norm enrich score: VC_SQRT normalized enrichment score.
(G) Heatmaps comparing changes in virtual 4C view of Rad21 HiChIP and H3K4me1 HiChIP signals between all HS-induced gene promoters and HS gained activated H3K4me3 enhancers (top) and HS-repressed gene promoters and HS decommissioned H3K4me3 enhancers (bottom). These enhancers are defined as described in Figure S1A. Viewpoint: promoters. Dynamic enhancers are ranked by distance from upstream to downstream of promoters. Only interactions within 500 kb are plotted. Norm enrich score: VC_SQRT normalized enrichment score.

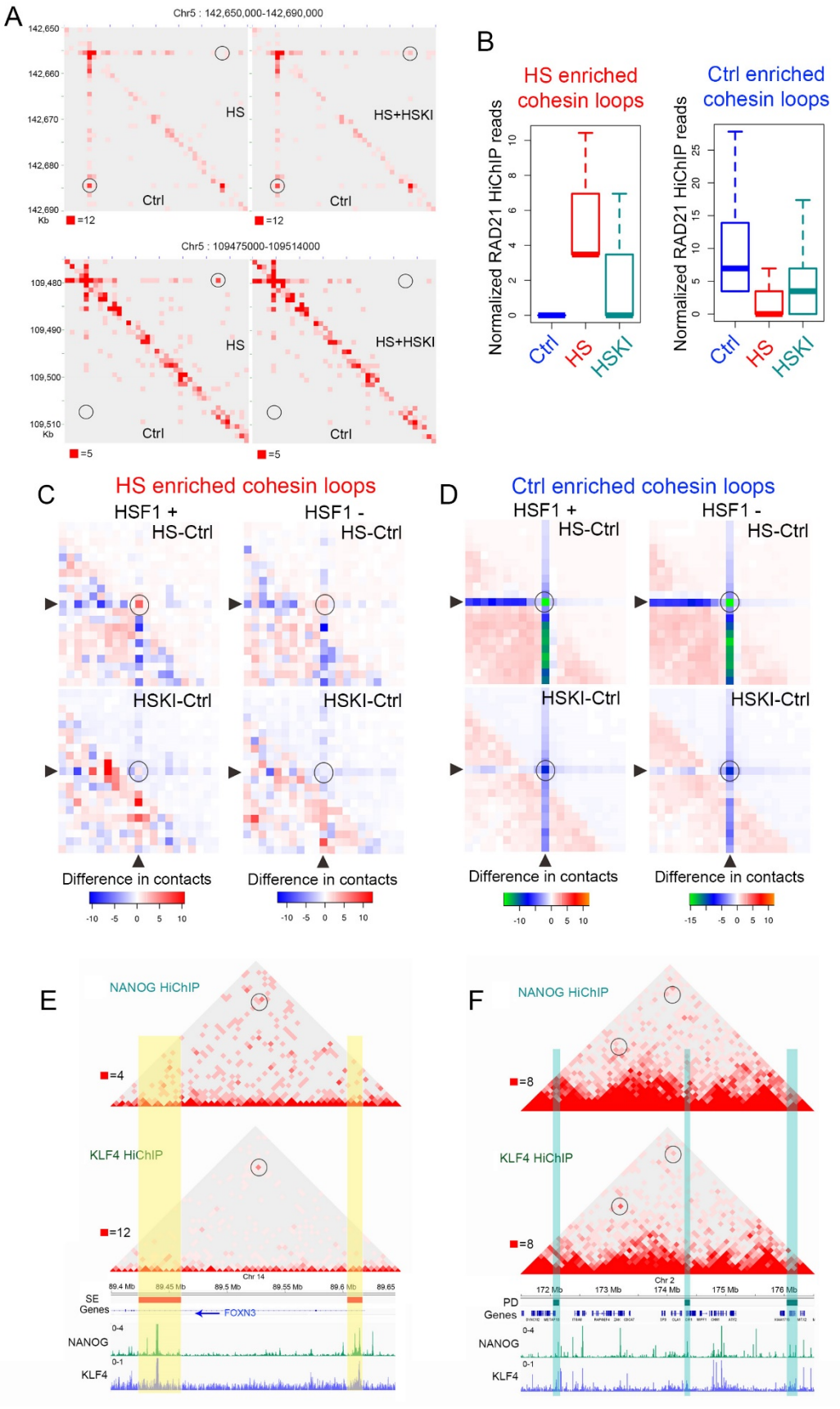
A
Chr5 : 142,650,000-142,690,000
142,650
142,660
142,670
142,680
142,690
Kb
HS
HS+HSKI
Ctrl
Ctrl
Ctrl
=12
=12
Chr5 : 109475000-109514000
109,480
109,490
109,500
109,510
Kb
HS
HS+HSKI
Ctrl
Ctrl
Ctrl
=5
=5
B
HS enriched cohesin loops
Ctrl enriched cohesin loops
Normalized RAD21 HiChIP reads
Normalized RAD21 HiChIP reads
Ctrl
HS
HSKI
Ctrl
HS
HSKI
C
HS enriched cohesin loops
HSF1 +
HS-Ctrl
HSF1 -
HS-Ctrl
HSKI-Ctrl
HSKI-Ctrl
Difference in contacts
Difference in contacts
-10 -5 0 5 10
-10 -5 0 5 10
D
Ctrl enriched cohesin loops
HSF1 +
HS-Ctrl
HSF1 -
HS-Ctrl
HSKI-Ctrl
HSKI-Ctrl
Difference in contacts
Difference in contacts
-10 0 5 10
-15 -5 0 5 10
E
NANOG HiChIP
=4
KLF4 HiChIP
=12
Chr 14
89.4 Mb
89.45 Mb
89.5 Mb
89.55 Mb
89.6 Mb
89.65
SE
Genes
FOXN3
NANOG
0-4
KLF4
0-1
F
NANOG HiChIP
=8
KLF4 HiChIP
=8
Chr 2
172 Mb
173 Mb
174 Mb
175 Mb
176 Mb
PD
Genes
NANOG
0-4
KLF4
0-1

Figure S5. Related to Figure 5.
(A) Juicebox browser views of Rad21 HiChIP in Ctrl, HS, and HS+KI in an example region (chr5:141.81-141.855 Mb) containing two Ctrl enriched Rad21 loops (top). A second region (chr5: 109,475,000-109,914,000) containing one HS enriched Rad21 loop (bottom). The HS induced changes are reversed by kinase inhibitors (HSKI).
(B) Boxplots quantifying changes observed in (A).
(C-D) Subtraction metaplots comparing HS-induced changes in Rad21 HiChIP contact frequency on all HS enriched (C) and Ctrl enriched loops (D) associated with HSF1 or not. HS effects are reversed by kinase inhibitors.
(E) NANOG HiChIP in the same region as Figure 5B.
(F) KLF4 HiChIP in the same region as Figure 5C.

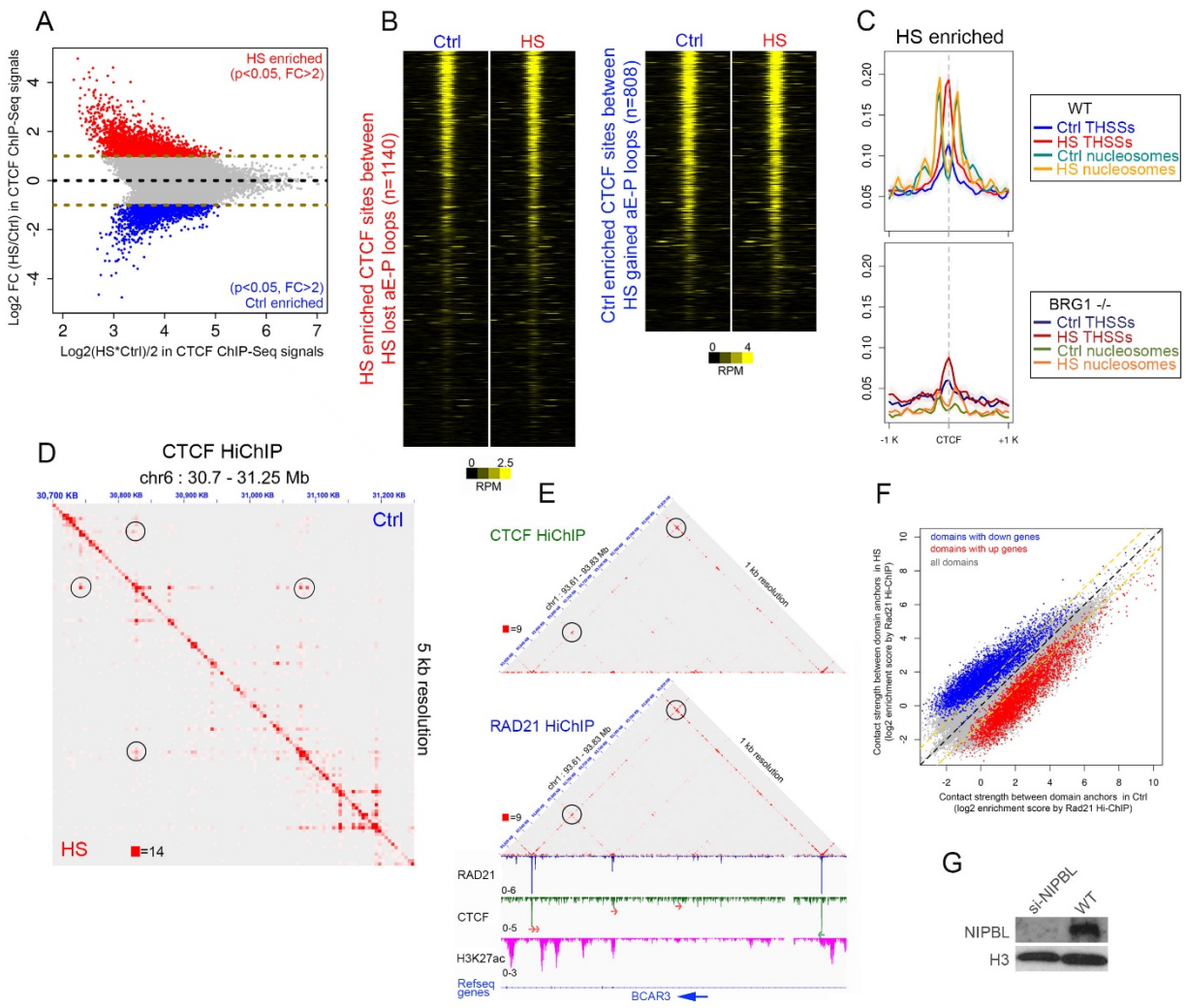

Figure S6. Related to Figure 6.

(A) Scatter plots showing MAnorm derived CTCF differential peaks in Ctrl and HS cells.

(B) Heatmaps comparing RAD21 ChIP-seq signals in control and temperature-stressed cells at the same CTCF site anchors used in Figure 6A. CTCF summits ± 1 kb are analyzed. RPM: reads per million per 50 bp bin.

(C) Average profiles of ATAC-seq THSSs and nucleosome signals using the same Y axis as in Figure S1A on HS gained enhancers in HS H9 cells (top) show no repositioning of phased nucleosomes and increased THSSs signals, suggesting increased binding of TFs after temperature stress. BRG1 knockout (bottom) results in absence of phased nucleosomes in both control and temperature stressed cells. Clusters derived by K-means clustering of nucleosomal reads.

(D) Browser view of normalized CTCF HiChIP contact matrices in Ctrl and HS cells showing Ctrl enriched and HS enrich CTCF loops in an example region on chr6.

(E) Comparison of read-normalized Rad21 and CTCF HiChIP in an example region on chr1. Region contains a CTCF loop showing a line indicative of cohesin extrusion. CTCF motif orientations labeled by red and green arrows.

(F) Average profiles comparing ATAC-seq nucleosomal and THSSs signals anchoring on HS enriched CTCF peaks in WT (top) and BRG1-/- (bottom) cells. Average signals per 50 bp bin per million reads are plotted.
(G) Western blot confirming the knockdown of NIPBL in H9 cells.

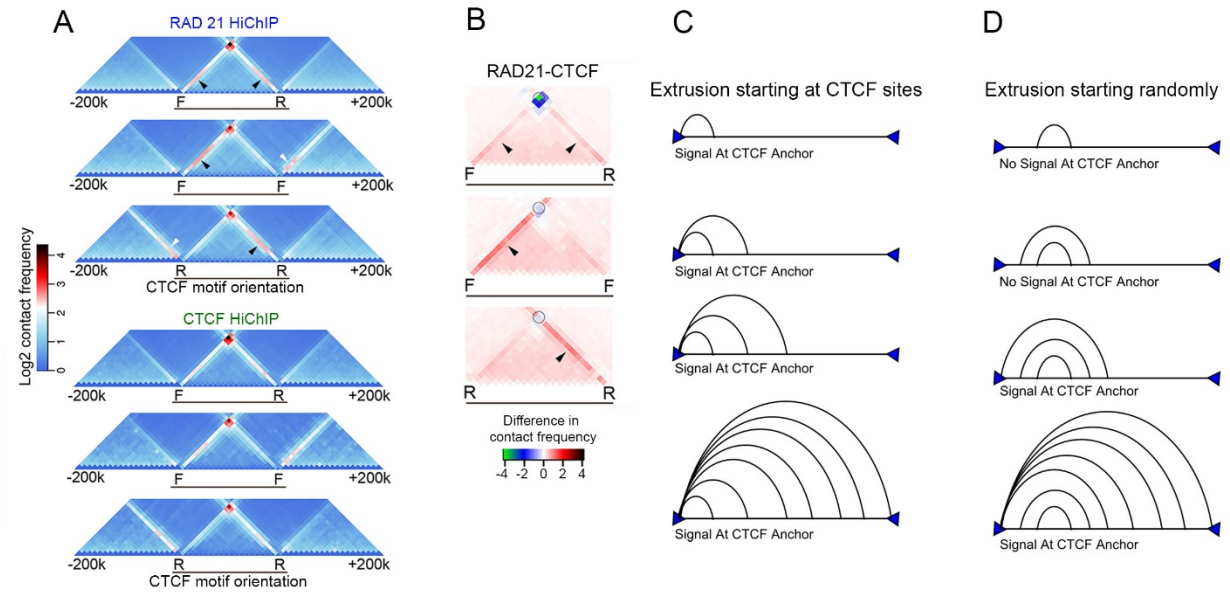

Figure S7. Related to Figure 7.
(A) Metaplots of CTCF HiChIP differ from metaplots of RAD21 HiChIP on F-R, F-F and R-R CTCF loops. Lines in RAD21 HiChIP suggest loop extrusion.
(B) Subtraction metaplots of RAD21 minus CTCF HiChIP contact frequency more clearly show observations in (A).
(C) Diagrams showing loop extrusion starting at CTCF sites.
(D) Diagrams showing loop extrusion starting at random sites.

Table S1. Summary of read numbers from ChIP-seq, ATAC-seq, and eU-seq experiments. Related to Figures 1, 2 and 6.

Experiment Description	Sample Name	Sequenced Read Pairs	mono-clonal mapped pairs
EU-seq	H9 EU-seq	68,877,895	8,765,137
EU-seq	HS H9 EU-seq	68,115,329	22,853,396
ATAC-seq	fast ATAC-seq Rep1	118,170,980	32,191,087
ATAC-seq	fast ATAC-seq Rep2	103,318,765	23,008,020
ATAC-seq	HS fast ATAC-seq Rep1	81,247,080	15,194,305
ATAC-seq	HS fast ATAC-seq Rep2	108,186,505	15,305,417
ATAC-seq	OMNI ATAC-seq	77,769,327	17,095,650
ATAC-seq	HS OMNI ATAC-seq	88,473,264	31,534,550
ATAC-seq	BRG1-KO_ATAC-seq	17,752,435	11,631,725
ATAC-seq	HS BRG1-KO_ATAC-seq	16,888,618	10,313,058
ChIP-Seq	RAD21 Rep1	18,008,195	14,999,514
ChIP-Seq	RAD21 Rep2	40,441,130	32,345,219
ChIP-Seq	HS RAD21 Rep1	18,008,554	15,159,520
ChIP-Seq	HS RAD21 Rep2	45,266,203	34,719,218
ChIP-Seq	CTCF	14,611,504	11,975,865
ChIP-Seq	HS CTCF	28,489,132	22,853,316
ChIP-Seq	ZNF143	42,930,894	35,069,243
ChIP-Seq	HS ZNF143	32,573,437	26,802,009
ChIP-Seq	RNAPII	23,839,421	19,220,900
ChIP-Seq	HS RNAPII	25,171,706	20,273,270
ChIP-Seq	RING1B	38,529,272	31,532,532
ChIP-Seq	HS RING1B	32,724,019	26,609,058
ChIP-Seq	c-FOS	30,423,826	24,644,202
ChIP-Seq	HS c-FOS	20,545,510	16,734,680
ChIP-Seq	BRG1	13,614,293	11,104,446
ChIP-Seq	HS BRG1	21,401,954	17,325,242
ChIP-Seq	HSF1	21,905,640	17,494,660
ChIP-Seq	HS HSF1	34,796,279	26,982,685
ChIP-Seq	HS KI HSF1	41,248,763	31,975,880
ChIP-Seq	OCT4	41,424,386	32,713,149
ChIP-Seq	HS OCT4	34,247,683	26,838,475
ChIP-Seq	NANOG	34,721,556	28,857,399
ChIP-Seq	HS NANOG	34,844,931	27,556,217
ChIP-Seq	KLF4	25,116,739	19,589,207
ChIP-Seq	HS KLF4	46,924,739	36,421,653
ChIP-Seq	WAPL	37,162,011	30,177,245

ChIP-Seq	HS WAPL	34,798,622	28,120,270
ChIP-Seq	NIPBL	39,164,024	31,920,922
ChIP-Seq	HS NIPBL	38,010,174	30,535,735
ChIP-Seq	H3K27ac Rep1	21,931,006	18,430,672
ChIP-Seq	H3K27ac Rep2	10,283,229	8,589,901
ChIP-Seq	HS H3K27ac Rep1	18,948,404	16,044,560
ChIP-Seq	HS H3K27ac Rep2	8,548,663	7,067,164
ChIP-Seq	H3K27me3	43,795,635	31,658,020
ChIP-Seq	HS H3K27me3	18,773,542	13,153,473
ChIP-Seq	H3K4me1	27,054,510	23,897,690
ChIP-Seq	HS H3K4me1	25,919,309	22,816,223
ChIP-Seq	H3K4me3	29,282,526	22,874,245
ChIP-Seq	HS H3K4me3	24,755,276	18,719,781
ChIP-Seq	BRG1-KO_H3K27ac	35,487,611	30,504,289
ChIP-Seq	HS BRG1-KO_H3K27ac	43,705,297	37,438,922
ChIP-Nexus	CTCF	60,977,193	36,060,441
ChIP-Nexus	HS CTCF	74,748,797	32,372,622
ChIP-Nexus	RAD21	35,345,131	7,866,284
ChIP-Nexus	HS RAD21	40,556,714	8,039,122

Table S2. Summary of quality control steps in the processing of sequencing reads obtained in HiChIP experiments. Related to Figures 3, 4, 5, 6, and 7.

Experiment Description	Sequenced Read Pairs	Unique Read Pairs	Hi-C Contacts
Rad21 HiChIP Rep1	327,840,789	159,720,637(48.72%)	108,201,694(33.00%/67.74%)
Rad21 HiChIP Rep2	87,010,131	58,823,169(67.60%)	39,516,875(45.42%/67.18%)
Rad21 HiChIP Rep3	124,188,827	83,606,395(67.32%)	55,755,324(44.90%/66.69%)
Rad21 HiChIP Rep4	63,500,514	16,073,568(25.31%)	10,049,359(15.83%/62.52%)
HS Rad21 HiChIP Rep1	250,139,434	179,543,527(71.78%)	114,541,662(45.79%/63.80%)
HS Rad21 HiChIP Rep2	93,931,067	72,090,933(76.75%)	47,673,797(50.75%/66.13%)
HS Rad21 HiChIP Rep3	149,416,527	98,323,089(65.80%)	65,807,224(44.04%/66.93%)
HS Rad21 HiChIP Rep4	68,920,318	28,067,253(40.72%)	17,737,471(25.74%/63.20%)
HS KI Rad21 HiChIP	119,333,012	69,397,925(58.15%)	49,721,948(41.67%/71.65%)
CTCF HiChIP Rep1	72,198,120	31,637,104(43.82%)	20,110,198(27.85%/63.57%)
CTCF HiChIP Rep2	13,114,778	7,831,995(59.72%)	5,273,728(40.21%/67.34%)
CTCF HiChIP Rep3	41,741,738	9,779,254(23.43%)	6,345,340(15.20%/64.89%)
HS CTCF HiChIP Rep1	74,134,921	27,741,206(37.42%)	19,557,316(26.38%/70.50%)
HS CTCF HiChIP Rep2	46,821,549	11,022,872(23.54%)	7,107,075(15.18%/64.48%)
OCT4 HiChIP Rep1	69,836,551	19,246,597(27.56%)	11,531,943(16.51%/59.92%)
OCT4 HiChIP Rep2	61,118,825	23,426,516(38.33%)	14,326,685(23.44%/61.16%)
HS OCT4 HiChIP Rep1	83,732,380	45,540,789(54.39%)	30,913,480(36.92%/67.88%)
HS OCT4 HiChIP Rep2	70,234,334	19,425,828(27.66%)	11,753,151(16.73%/60.50%)
NANOG HiChIP Rep1	100,382,818	68,276,347(68.02%)	47,127,026(46.95%/69.02%)
NANOG HiChIP Rep2	4,057,332	3,292,918(81.16%)	1,966,789(48.47%/59.73%)
HS NANOG HiChIP Rep1	92,153,040	62,986,031(68.35%)	43,644,215(47.36%/69.29%)
HS NANOG HiChIP Rep2	5,473,361	4,640,723(84.79%)	2,662,956(48.65%/57.38%)
KLF4 HiChIP Rep1	121,964,602	54,776,012(44.91%)	30,245,124(24.80%/55.22%)
KLF4 HiChIP Rep2	8,849,661	7,040,063(79.55%)	3,770,032(42.60%/53.55%)
HS KLF4 HiChIP	92,095,681	57,369,824(62.29%)	29,653,453(32.20%/51.69%)
H3K4me1 HiChIP Rep1	53,487,872	30,661,397(57.32%)	19,331,303(36.14%/63.05%)
H3K4me1 HiChIP Rep2	82,380,337	40,438,143(49.09%)	25,289,140(30.70%/62.54%)
HS H3K4me1 HiChIP Rep1	96,801,462	31,396,227(32.43%)	19,622,945(20.27%/62.50%)
HS H3K4me1 HiChIP Rep2	112,042,918	35,105,011(31.33%)	21,773,542(19.43%/62.02%)
siNIPBL HS CTCF HiChIP	56,100,419	17,040,451(30.37%)	8,819,287(15.72%/51.76%)
siNIPBL HS H3K4me1 HiChIP	74,434,067	62,070,947(83.39%)	36,004,478(48.37%/58.01%)